Photon Structure Functions at LEP by L3

Maria Novella Kienzle-Focacci

DPNC, Geneva University, Switzerland

E-mail: maria.kienzle@cern.ch

Abstract

The reactions $e^+e^- \to e^+e^- l^+l^-$ and $e^+e^- \to e^+e^- hadrons$, in a single and double tag configurations, are studied at LEP with the L3 detector. The data correspond to a total integrated luminosity of 140 pb^{-1} at $\sqrt{s} = 91$ GeV, and 52 pb^{-1} at $\sqrt{s} = 183$ GeV; they cover a Q^2 range $1.4 < Q^2 < 500$ GeV^2. The leptonic photon structure function F_2^γ and azimuthal correlations are measured for $e^+e^- \to e^+e^- \mu^+\mu^-$. The related structure functions F_A^γ and F_B^γ are determined, the non-zero value of F_A^γ implies the presence of a small longitudinal photon amplitude. Results on the hadronic F_2^γ are presented in the range $0.002 < x < 0.5$ and compared to existing QCD parametrizations. For $x < 0.2$ the data are above the predictions of GRV and SaS parametrisations and F_2^γ increases with $\ln Q^2$ faster than expected. Both observations indicate that the gluon content in the photon is at present underestimated. Double tag events are also analysed and compared to BFKL inspired calculations.

1 Introduction

The data have been collected at LEP from 1991 to 1995 at $\sqrt{s} \simeq 91$ GeV and in 1997 at $\sqrt{s} = 183$ GeV. The detailed description of the L3 detector can be found in Ref. [1]. The deep inelastic $e^+e^- \to e^+e^- X$ two-photon reaction is selected by detecting one or both scattered electrons in the forward electromagnetic calorimeters. For single tag events only one electron must be seen and no other electron candidate must be present in the detector (anti-tag condition). The kinematical x and Q^2 ranges and the corresonding number of events are listed in table 1. As usual, Q is the mass of the probe photon and $x = \frac{Q^2}{Q^2+P^2+W_{\gamma\gamma}^2}$, where P is the mass of the target photon and $W_{\gamma\gamma}$ the mass of the two-photon system.

To simulate QED processes we have used DIAG36 [7] which calculates to $O(\alpha^4)$ the full set of QED diagrams and JAMVG [8], which has exact calculations only for the multiperipheral diagram. We check the influence of initial state radiations with the generator RADCOR [9]. These generators estimate also the $e^+e^- \to e^+e^- \tau^+\tau^-$ background. For the hadronic channels we have used TWOGAM [10], PHOJET [11] and HERWIG [12]. The hadronisation parameters of these generators were not specifically tuned to our two-photon data. The backgrounds from annihilation processes are estimated with the generators KORALZ [13] and PYTHIA [14]. All MC events are passed through a full detector simulation [15] and they are analysed as the data.

Channel	$\sqrt{s}$ (GeV)	Q^2 (GeV^2)	x	NeV	L$_{ee}$ (pb^{-1})	Ref.
Single Tag						
e^+e^-	91	1.4-7.6	0-1.	3802	93.7	[2]
$\mu^+\mu^-$	91	1.4-7.6	0-1.	7152	93.7	[2]
hadrons	91	1.2-3.	0.002-0.1	5772	140.	[3]
		3.-9.	0.005-0.2	4156		
hadrons	91	40.-500.	0.05-0.98	406	140.	[4]
hadrons	183	9.-13.	0.01-0.3	632	51.9	[5]
		13.-18.	0.01-0.5	477		
		18.-30.	0.01-0.5	540		
Double Tag						
hadrons	91	1.2-9.		137	140.	[6]
	183	9.-30.		34	51.9	

Table 1: Number of single and double tagged events, selected as two-photon interactions $e^+e^- \to e^+e^-X$.

2 The leptonic structure functions

The leptonic structure function, $F_2^\gamma(x)$, obtained in the reaction $e^+e^- \to e^+e^-\mu^+\mu^-$ [2], is shown in Fig.1a.

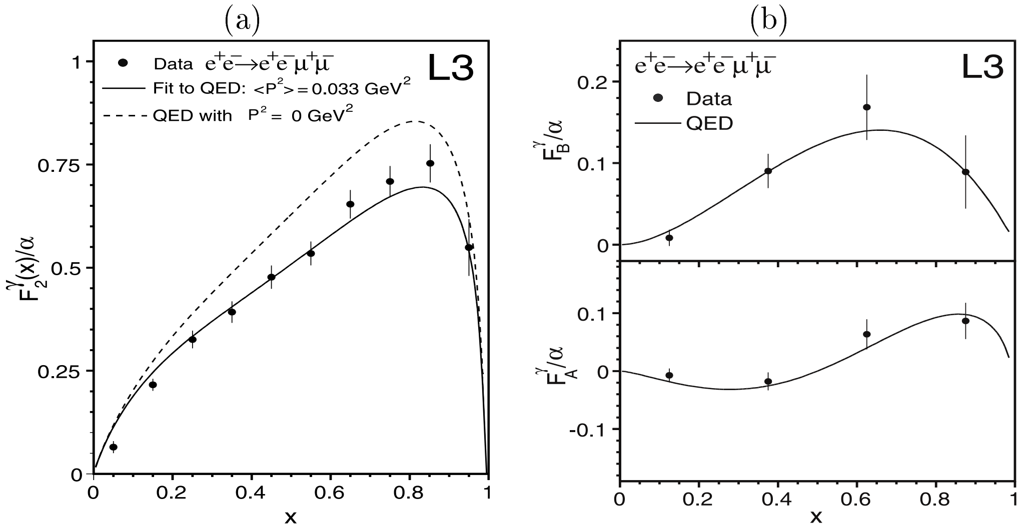

Figure 1: Leptonic structure functions obtained at $\sqrt{s}$=91 GeV.

If the target photon is assumed to be real ($P^2 = 0$), the QED prediction for $F_2^\gamma(x)$ is significantly higher than the measured values ($\chi^2/dof = 10.7$). By leaving P^2 as a free parameter in a QED fit to the data, we obtain a mean value $< P^2 >= 0.033 \pm 0.005$ GeV^2 ($\chi^2/dof = 1.7$). This is in excellent agreement with the value of 0.034 ± 0.002 GeV^2 calculated by the Monte Carlo including radiative corrections [9]. Without radiative corrections the expected mean virtuality of the target photon is $< P^2 >= 0.024 \pm 0.003$, two standard deviations below the measurement.

In the two-photon center of mass, we measure the polar, $\theta^\star$, and azimuthal, χ, angle of the muon pair. The azimuthal angle distibution is studied in the range $| \cos\theta^\star | \leq 0.7$, a region where the detector efficiency is uniform and the sensitivity to longitudinal and transverse photon interference is high. The data, subdivided in four x intervals, are well fitted by the form

$$dN/d\chi = A_1(x) + A_2(x)\cos\chi + A_3(x)\cos 2\chi \qquad (1)$$

The coefficients A are related to the polarization of the two virtual photons. To determine the structure functions $F_A \propto A_2$ and $F_B \propto A_3$, the measurement is extrapolated to the full $\cos\theta^\star$ interval. The results are shown in Fig.1b together with the QED expectations. The interference term of the longitudinal photon, measured by the structure function F_A, is small, but significantly non-zero.

3 The hadronic structure function F_2^γ

For the hadronic structure function measurement the x variable must be determined from the effective mass, $W_{\rm vis}$, of all detected particles. The value $W_{\rm vis}$ is lower than $W_{\gamma\gamma}$, due to the limited detector acceptance. We optimize this measurement by including all particles, also those observed in the forward calorimeters, and by using the constraint of the transverse momentum conservation as suggested in the LEP2 workshop:

$$W^2_{rec} \equiv (p_+^{e_{in}} - p_+^{e_{tag}})(\sum_i p_-^i) - |p_t^{e_{tag}}|^2 \qquad p_\pm \equiv E \pm p_z. \qquad (2)$$

The improvement due to this algorithm is demonstrated in Fig.3a.

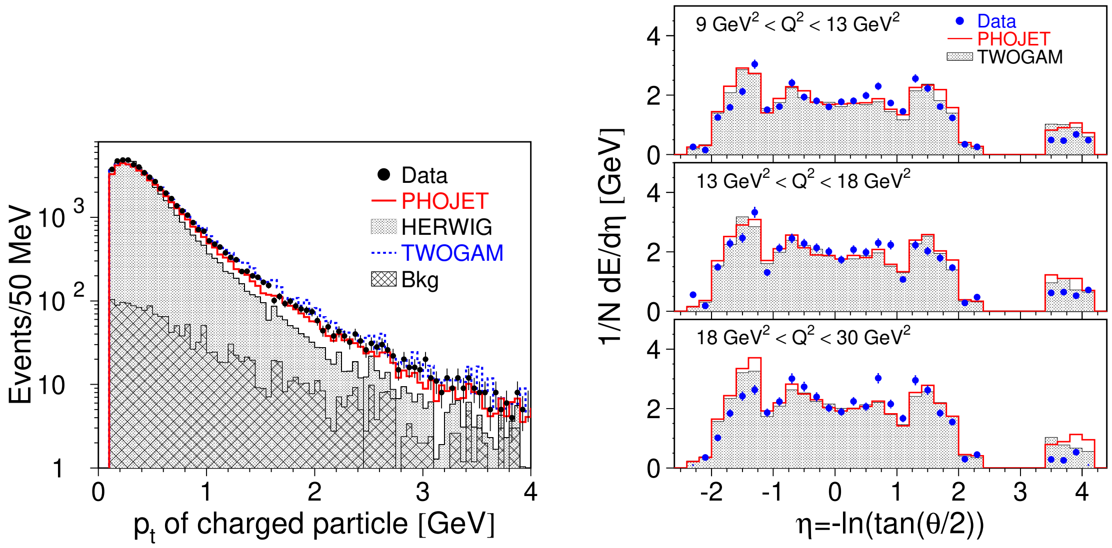

(a) (b)

Figure 2: Data at $\sqrt{s}$=183 GeV. a) Transverse momentum of charged particles, b) Energy flow of all particles entering in the effective mass calculation.

To go from the measured x_{rec} to x we use an unfolding matrix [16] given by Monte Carlo. It is therefore extremely important that the Monte Carlo reproduce the particles distributions observed in the detector. We have compared the data to HERWIG, PHOJET and TWOGAM, two examples are shown in Fig.2. We conclude that HERWIG distributions are not compatible with the data while PHOJET and TWOGAM are satisfactory. At the lowest values of Q^2 and x we observe (Fig.3b) a large variation of F_2^γ

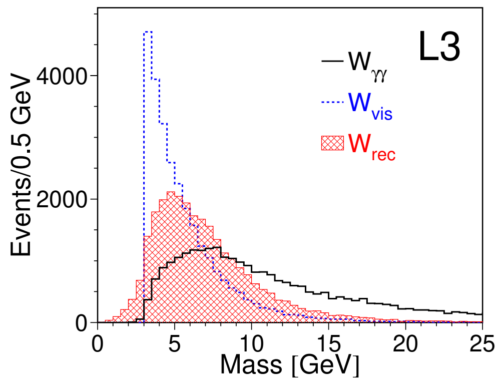

(a)

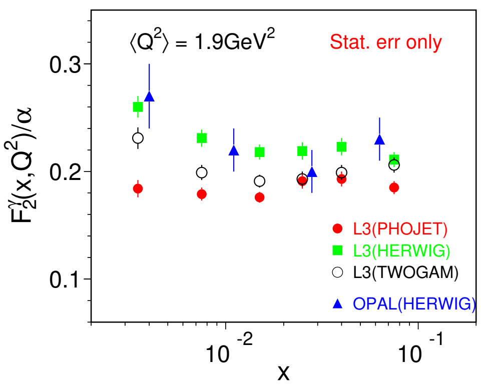

(b)

Figure 3: a) The distributions of $W_{\rm vis}$, $W_{\rm rec}$ and $W_{\gamma\gamma}$ given by PHOJET. b) At low x and Q^2, F_2^γ depends on the Monte Carlo used to unfold the data. By using HERWIG, which doesn't fit well the observed distributions, L3 obtain the same results as OPAL (only statistical errors are considered)

depending on the Monte Carlo model used to correct the data. In Fig.3b we show also that the results of OPAL [17] are very similar to ours, if the same Monte Carlo is used. This demonstrates the importance, for the LEP experiments, to use the same generators, provided that the agreement with the data is found satisfactory.

For low Q^2 we give separately the values of F_2^γ unfolded with PHOJET and TWOGAM (Fig.4a), for the higher Q^2 ranges the two values are very similar, PHOJET is used and the difference with TWOGAM is included in the systematic error (Fig.4b). The data agree with the QCD parametrisation of GRV and SAS for $x > 0.1$, the region were the parametrisations were fitted to previous data, but at low x the measured values of F_2^γ are higher than expected. Notice that the virtuality of the target photon is neglected in the predictions shown in Fig.4, by taking this into account the discrepancy with the data would increase.

The analysis of the events with an electron detected in the endcap calorimeters covers the full x range for $40 < Q^2 < 500$ GeV^2. The data are well reproduced by the $\gamma^*\gamma^* \to \mathrm{q\bar{q}}$ diagram (QPM) except at low values of x where it is necessary to take into account the partonic structure of the photon; the GRV parametrisation shows here a good agreement with the data (Fig.5a).

The rise of F_2^γ with $\ln Q^2$ is measured in the range $0.01 < x < 0.1$ (Fig.5b). A fit to the data of the form $a + b \ln Q^2$ gives a slope $b = 0.080 \pm 0.009 \pm 0.009$, where the first error includes the statistical and systematic error of the experiment and the second the Monte Carlo unfolding effects. The slope value is higher than expected by GRV-HO ($b = 0.061$) and SAS-1d ($b = 0.043$).

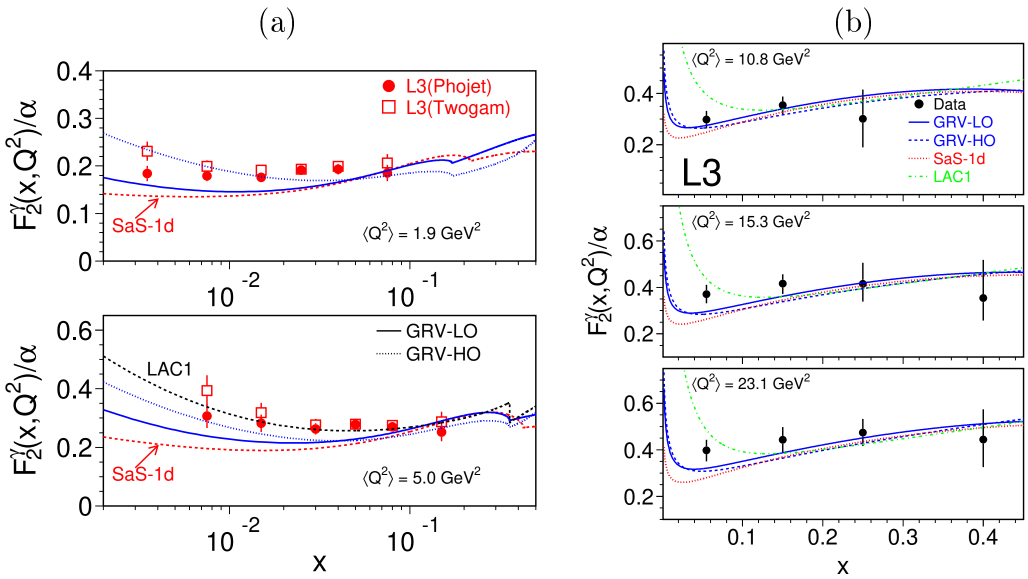

Figure 4: F_2^γ results compared to different QCD predictions. a) Data at $\sqrt{s}$=91 GeV. b) Data at $\sqrt{s}$=183 GeV. (Statistical and systematic errors are added in quadrature)

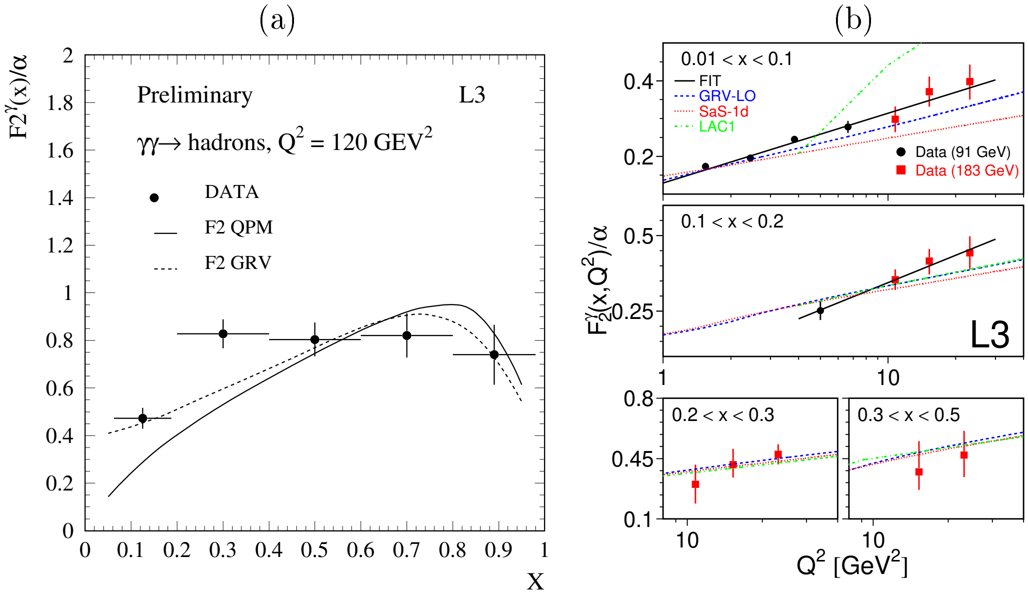

Figure 5: a) Data at $\sqrt{s}$=91 GeV for $40 < Q^2 < 500$ GeV^2, the electron is tagged in the detector endcaps. The errors are only statistical. b) F_2^γ as function of $\ln Q^2$. Statistical and systematic errors are added in quadrature.

4 Double tag

In some event both electrons are measured in the forward calorimeters (table 1). Attention to this channel was recently rised [18, 19] because the $\gamma^*\gamma^*$ cross section provides a clean test of BFKL [20] calculations. The cross-section of two virtual photon collisions in leading order approximation can be expressed as :

$$\sigma_{\gamma\gamma} = \sigma_0 \left(\frac{s}{s_0}\right)^{\alpha_P - 1} \approx \sigma_0 \left(\frac{W_{\gamma\gamma}^2}{\sqrt{Q_1^2 Q_2^2}}\right)^{\alpha_P - 1} \quad , \quad s_0 = \frac{\sqrt{Q_1^2 Q_2^2}}{y_1 y_2} \tag{3}$$

This form is analogous to the one obtained by Regge trajectories, but the Pomeron intercept α_P, which is calculable ($\alpha_P - 1 = (4/\pi \ln 2) N_c \alpha_s$), has a value $\alpha_P \simeq 1.53$, much larger than the soft Pomeron intercept value of $\simeq 1.079$, obtained by universal total cross-sections fits [21].

The experimental distributions of double tag events are well reproduced by the same event generators used for single-tag events. In order to compare the measured cross-sections to the BFKL model [18] we restrict the kinematical interval to $Q_i^2 \geq 2.5$ GeV^2, $y_i \geq 0.1$ and $2 \leq \ln(s/s_0) \leq 6$, thus obtaining 12 events at $\sqrt{s}$ =91 GeV and 9 events at $\sqrt{s}$= 183 GeV. The cross-sections are given in table 2, with statistical and systematic errors. We find a good agreement with the Monte Carlo TWOGAM and PHOJET absolute value predictions; QPM is insufficient to describe the data, but present BFKL predictions [22] are more than a factor 10 larger than the experimental values.

E_{beam}	Data	QPM	1-gluon	BFKL	TOWGAM	PHOJET
[GeV]	[pb]	[pb]	[pb]	[pb]	[pb]	[pb]
91	$0.084 \pm 0.026 \pm 0.005$	0.032	0.200	2.829	0.089	0.066
183	$0.17 \pm 0.07 \pm 0.01$	0.018	0.135	2.135	0.28	0.25

Table 2: The double tag cross-sections in the kinematic region defined in the text at $\sqrt{s} \simeq 91$ GeV and $\sqrt{s} \simeq 183$ GeV, compared to the predictions of QPM, one-gluon exchange, BFKL and Monte Carlo models. The first error on the data is statistical and the second is systematic.

5 Conclusions

At LEP we obtain high statistics samples of two-photon events with very low background contamination. More data are expected, for a total integrated luminosity of $L_{ee} \simeq 150$ pb^{-1} in 1998 and $L_{ee} \simeq 200$ pb^{-1} in 1999-2000.

The precision of the measurement of the hadronic photon structure function F_2^γ is at present limited by the Monte Carlo models at low values of x and Q^2. Although some MC reproduces well most of the experimental distributions, more effort is still required on the understanding of the many processes contributing to two-photon interactions. The use of present LEP data can improve the parametrisations of the partonic content of the photon; the data show that the gluon contribution is probably underestimated.

Double tag events do not show the high increase of the cross-section, expected by the recent BFKL inspired models.

6 Acknowledgements

The present results are the fruit of the excellent performance of the LEP machine and of the good collaboration of all members of the L3 two-photon analysis group. This analysis is the work of C.H.Lin, F.Erne and G.Susinno.

References

[1] L3 Collaboration, B.Adeva et al., Nucl. Inst. Meth. **A 289** (1990) 35.

[2] L3 Collaboration, M.Acciari et al., CERN-EP/98-060 to be published in Phys. Lett. and G. Susinno, PhD thesis 2961, Université de Genève, 1997.

[3] L3 Collaboration, M.Acciari et al., CERN-EP/98-098 to be published in Phys. Lett.

[4] F.Erne, Ascona L3 meeting (june 1998)

[5] C.H.Lin, L3 Note 2298 (1998)

[6] C.H.Lin, L3 Note 2338 (1998)

[7] DIAG36 : F.A.Berends,P.H.Daverfeldt and R.Kleiss, Nucl. Phys. **B 253** (1985) 441 and Comp. Phys. Comm. **40** (1986) 285.

[8] JAMVG : J.Vermaseren, Nucl. Phys. **B 229** (1983) 347.

[9] RADCOR : F.A.Berends,P.H.Daverfeldt and R.Kleiss,, Nucl. Phys. **B 253** (1985) 421. and Comp. Phys. Comm. **40** (1986) 271.

[10] TWOGAM ver. 1.71 is used : S. Nova et al., DELPHI Note 9–35 (1990).

[11] PHOJET ver. 1.05c is used : R. Engel and J. Ranft, Phys. Rev. **D54** (1996) 4244.

[12] HERWIG ver. 5.9 is used : G. Marchesini et al.,Comp. Phys. Comm. **67** (1992) 465.

[13] KORALZ : S.Jadach, B.F.L.Ward and Z.Was, Comp. Phys. Comm. **79** (1994) 503, KORALW : M.Skrzypek,S.Jadach, W.Placzek and Z.Was, Comp. Phys. Comm. **94** (1996) 216.

[14] PYTHIA : T. Sjöstrand, Comp. Phys. Comm. **82** (1994) 74.

[15] R.Brun et al., GEANT 3.15 preprint CERN DD/EE/84-1 (Revised 1987).

[16] G. D'Agostini, Nucl. Inst. Meth. **A 362** (1995) 487.

[17] OPAL coll., K.Ackerstaff et al., Phys. Lett. **B 412** (1997) 225.

[18] J. Bartels, A. De Roeck and H. Lotter, Phys. Lett. **B 389** (1996) 742;
J. Bartels, A. De Roeck, C. Ewerz and H. Lotter, hep-ph/9710500

[19] S.J. Brodsky, F. Hautmann and D.E. Soper, Phys. Rev. Lett. **78** (1997) 803;
S.J. Brodsky, F. Hautmann and D.E. Soper, Phys. Rev. **D 56** (1997) 6957.

[20] L.N. Lipatov, Sov. J. Nucl. Phys. **23** (1976) 338; E.A. Kuraev, L.N. Lipatov and V.S. Fadin, Sov. Phys. JETP **45** (1977) 199; I. Balitskii and L.N. Lipatov, Sov. J. Nucl. Phys. **28** (1978) 822.

[21] Review of Particle Physics, Phys. Rev. **D 54** (1996) 192.

[22] We thank A. De Roeck for giving us the predictions of one-gluon exchange and BFKL models in our kinematical range.